AGU ADVANCING EARTH AND SPACE SCIENCES

Geophysical Research Letters®

RESEARCH LETTER
10.1029/2023GL105640

Higher Exposure of Poorer People to Emerging Weather Whiplash in a Warmer World

Boen Zhang[1], Shuo Wang[1,2], Jakob Zscheischler[3], and Hamid Moradkhani[4,5]

[1]Department of Land Surveying and Geo-Informatics, The Hong Kong Polytechnic University, Hong Kong, China, [2]Research Institute for Land and Space, The Hong Kong Polytechnic University, Hong Kong, China, [3]Department of Computational Hydrosystems, Helmholtz Centre for Environmental Research–UFZ, Leipzig, Germany, [4]Department of Civil, Construction, and Environmental Engineering, University of Alabama, Tuscaloosa, AL, USA, [5]Center for Complex Hydrosystems Research, University of Alabama, Tuscaloosa, AL, USA

Abstract The emergence of abrupt shift from drought to downpour has attracted widespread attention in recent years, with particularly disastrous consequences in low-income regions. However, the spatiotemporal evolution and poverty exposure to such drought-to-downpour events remain poorly understood. Here, we investigate the connection between poverty and drought-to-downpour events based on three data products and climate models on a global scale. We find that the drought-to-downpour events increased by 24%–48% in the poorest 20% of the world's population from 1980 to 2010. The drought-to-downpour events do not appear to be occurring more frequently in most regions globally, just affecting regions with higher poverty rates more frequently, especially in African countries. The exposure inequality remains under future socioeconomic pathways, with a nearly fivefold increase in the exposure for the poorer populations. Poverty exposure to more frequent drought-to-downpour events demands greater support for climate adaptation in low-income countries to reduce poverty and inequality.

Plain Language Summary Many regions have suffered greatly from recent occurrences of abrupt shift from drought to downpour, suggesting that the emerging threat is a global challenge. Such drought-to-downpour events pose challenges to water infrastructures in developed countries, let alone those poor countries with limited adaptation capacity and resources. However, the connection between the drought-to-downpour events and poverty incidence remains poorly understood. Here, we show that such drought-to-downpour events experienced by the poorest 20% of the world's population increased significantly by 24%–48% from 1980 to 2010. Such a significant increase, however, is not observed for the remaining wealthiest 80%. The drought-to-downpour events do not appear to be occurring more frequently in most global regions, just affecting regions with higher poverty rates more frequently, especially in African countries. Climate projections show that such inequality would remain in a warming climate. Our results highlight the urgency to provide greater support for climate adaptation in low-income countries to reduce poverty and inequality.

Boen Zhang and Shuo Wang contributed equally to this work.

Key Points:

- The connection between poverty incidence and drought-to-downpour weather whiplashes is uncovered on a global scale
- The drought-to-downpour events increased by 24%–48% in the poorest 20% of the world's population from 1980 to 2010
- The drought-to-downpour events do not appear to be occurring more frequently in most global regions, just affecting regions with higher poverty rates more frequently

Supporting Information:

Supporting Information may be found in the online version of this article.

Correspondence to:

S. Wang,
shuo.s.wang@polyu.edu.hk

Citation:

Zhang, B., Wang, S., Zscheischler, J., & Moradkhani, H. (2023). Higher exposure of poorer people to emerging weather whiplash in a warmer world. *Geophysical Research Letters*, *50*, e2023GL105640. https://doi.org/10.1029/2023GL105640

Received 24 JUL 2023
Accepted 13 OCT 2023

Author Contributions:

Conceptualization: Shuo Wang
Data curation: Boen Zhang
Formal analysis: Boen Zhang, Shuo Wang
Funding acquisition: Shuo Wang
Investigation: Shuo Wang
Methodology: Boen Zhang
Project Administration: Shuo Wang
Resources: Shuo Wang
Software: Boen Zhang
Supervision: Shuo Wang
Validation: Boen Zhang
Visualization: Boen Zhang

1. Introduction

Poor countries or individuals often pay the heaviest price for climate extreme events (e.g., heatwaves, droughts, and floods) because they are often ill-equipped to adequately prepare for these extreme events and struggle harder to recover from them afterward (Ahmadalipour, Moradkhani, Castelletti, & Magliocca, 2019; Ahmadalipour, Moradkhani, & Kumar, 2019; Callahan & Mankin, 2022; Gazzotti et al., 2021; Wing et al., 2022). Such extreme events are very likely to become more frequent and intense under a warming climate, thereby increasing the already daunting costs of adaptation for low-income countries in coming decades (Batibeniz et al., 2020; Masood et al., 2022; Swain et al., 2018). In addition to individual extreme events, the emergence of compound events such as the abrupt shift from drought to downpour (hereafter referred to as drought-to-downpour) has been receiving widespread attention from researchers, practitioners, and policy makers (Zscheischler et al., 2018, 2020). Recent drought-to-downpour events in multiple countries such as India (Roxy et al., 2017), Peru (Son et al., 2020), Mozambique (Brida et al., 2013), the United Kingdom (Parry et al., 2013), and the United States (Simon Wang et al., 2017) illustrate that the emerging threat is a global challenge. This is especially true in low-income countries where infrastructure systems tend to be less developed and the multi-hazard early warning system is often lacking, the drought-to-downpour events can cause unmitigated damage and suffering (Hallegatte & Rozenberg, 2017).

Writing – original draft: Boen Zhang, Shuo Wang
Writing – review & editing: Jakob Zscheischler, Hamid Moradkhani

Poverty exposure to single climate extreme events has been well documented (Baez et al., 2020; Rentschler et al., 2022; Winsemius et al., 2018). Among the top 10 countries in terms of the impacts of climate extreme events in 2019, eight are lower-middle-income countries according to the Global Climate Risk Index 2021 (Eckstein et al., 2021). Approximately 170 million people worldwide are exposed to 1-in-100-year floods and living in extreme poverty, nearly half of which reside in Sub-Saharan Africa (Rentschler et al., 2022). In addition, studies show that poor people are often disproportionately exposed to droughts (Winsemius et al., 2018), floods (Rentschler et al., 2022), and heatwaves (King & Harrington, 2018). Yet, none of existing studies consider the interrelationship between poverty incidence and compound climate events, especially the drought-to-downpour events that have attracted worldwide attention (Chen & Wang, 2022; Qing et al., 2023; You et al., 2023). Such events often exacerbate damage due to the compounding effects of multiple hazards and are likely to have the most devastating impacts on low-income countries (He & Sheffield, 2020).

Recognizing the severe impacts of the drought-to-downpour events on socioeconomic development, developed countries have made a multibillion-dollar investment for constructing new water infrastructures such as levee setback projects (Collenteur et al., 2015). In comparison, current water infrastructure in low-income countries is typically designed for individual water-related hazards (i.e., drought or rainstorm) and often undersized, failing to address hazards from the drought-to-downpour events (Rentschler et al., 2022; Simon & Leck, 2015). To reduce such an inequality, the 27th Conference of the Parties to the United Nations Framework Convention on Climate Change (COP27) reached an agreement to compensate vulnerable developing countries for loss and damage from climate extreme events (Masood et al., 2022). However, the exposure risk of emerging drought-to-downpour events remains poorly understood, especially in low-income countries, which may cause inappropriate investment in water infrastructure of developing countries and potentially increase risks of infrastructure failure in the future, thereby reverting years of progress in development and poverty reduction. Therefore, it is urgent and vital to conduct a global assessment of drought-to-downpour events, including their recent evolution in low-income countries and regions, hot spots of exposure, and the inequality in exposure, enhancing climate resilience for low-income countries.

2. Methods

Gridded data products of daily precipitation are taken from three data sets, including the Rainfall Estimates on a Gridded Network (REGEN) (Contractor et al., 2019), the ERA5 reanalysis (Hersbach et al., 2020), and Princeton University's global land surface model data (Sheffield et al., 2006) to investigate global drought-to-downpour events from 1955 to 2014 (see a detailed description and evaluation of the three data sets in Text S1 as well as Figures S22, S23, and S24 in Supporting Information S1). Here, a drought-to-downpour event is defined as the occurrence of downpour within a month after the last month of a drought event (see a schematic in Figure S1 in Supporting Information S1). Drought is defined as the monthly self-calibrating Palmer Drought Severity Index (scPDSI) values continuously below −2 for at least three months. The monthly potential evapotranspiration (PET) in the Climate Research Unit (CRU) data set is used to calculate the scPDSI (Harris & Jones, 2020). The downpour is defined as the daily precipitation amount exceeding two thresholds: the 95th and 99th percentiles of precipitation on wet days (i.e., daily rainfall of at least 1 mm). A sensitivity analysis on the choice of drought threshold and precipitation quantile can be found in Text S2 in Supporting Information S1. In addition to data products, climate simulation data sets from 15 CMIP5 and 10 CMIP6 model outputs (Tables S1 and S2 in Supporting Information S1) as well as CESM Large Ensemble Community Project (CESM-LENS) are used to identify drought-to-downpour events under historical and future climates (Deser et al., 2020). Future climate projections under two emission scenarios (RCP4.5 and RCP8.5) are used. The monthly PET is also estimated based on the climate model simulations using the corrected Penman-Monteith equation, which takes into account atmospheric CO_2 concentration (Yang et al., 2019). The climate model simulation data sets are regridded onto $2.5° \times 2°$ grids given their coarse resolutions.

To estimate the poverty exposure of drought-to-downpour events, we use a 5-arcmin gridded subnational data set of GDP per capita (PPP, i.e., purchasing power parity) from Kummu et al. (2020) to group the globe into two clusters (i.e., the poorest 20% and the wealthiest 80%). This data set provides average GDP per capita at the subnational level for the 25-year period of 1990–2015, which is generated through compiling the reported data at national and subnational scales, together with temporal interpolation and extrapolation (Figure S13 in Supporting Information S1). The population exposure is determined based on the population density in World Pop 2000 maps

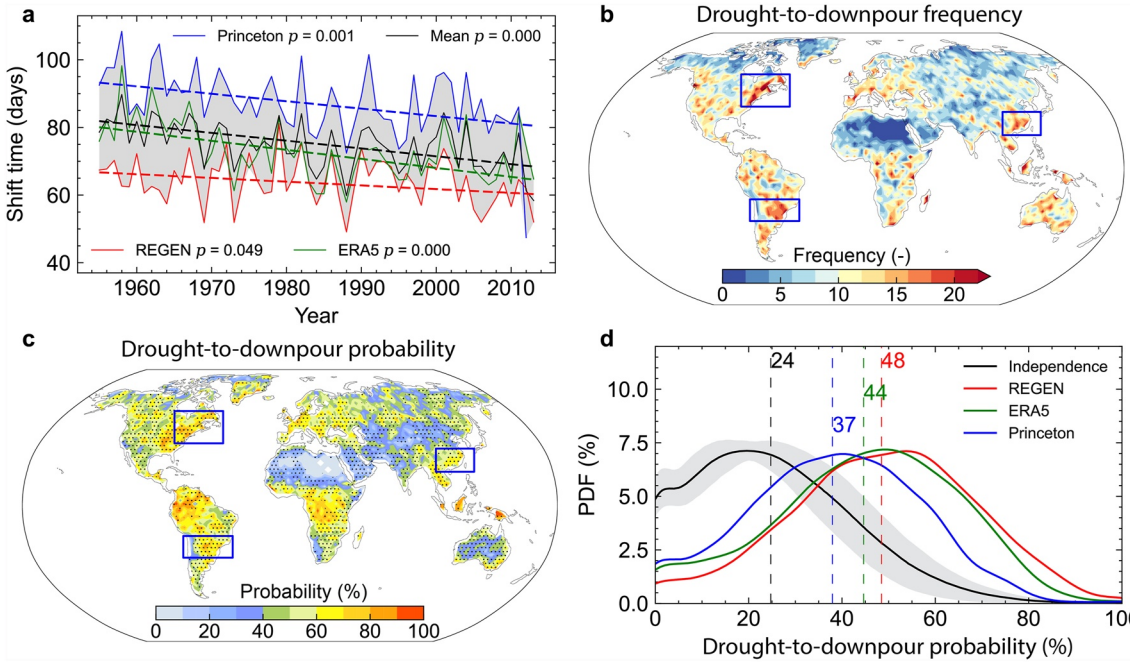

Figure 1. (a) Temporal evolution of the transition time from droughts to R95p downpours generated from three data products (REGEN, ERA5, and Princeton). Solid lines represent annual values of the global land-averaged transition time and dashed lines represent the linear trend based on the Sen's slope estimator (Sen, 1968). The *p*-value is the trend significance using a Mann–Kendall (MK) test (Kendall, 1975). The shaded areas represent the spread in the three data products. The historical (b) frequency and (c) probability of abrupt shift from droughts to R95p downpours within a month over the period of 1955–2014. The drought-to-downpour probability is calculated as the percentage of drought events that abruptly shift to downpours within a month. The stippling in (c) indicates the drought-to-downpour probability is significantly higher than expected from independence between drought and downpour occurrences. (d) PDF of the land fraction showing the drought-to-downpour probability generated from data products and 1,000 synthetic data sets that assume independence between drought and downpour occurrences. The vertical dashed lines represent the global mean drought-to-downpour probability. The lower and upper bounds of the gray shading in (d) refer to 2.5th and 97.5th percentile estimates, respectively.

calibrated on census and satellite data (WorldPop, 2020). In addition, we use the poverty rates available in the latest edition of the World Bank's Global Subnational Atlas of Poverty (GSAP) (World Bank, 2021). Here, we use the poverty headcount ratio (%) at $5.50 per day, which is one of the standard World Bank definitions of poverty (Figure S12 in Supporting Information S1). Since there are small subnational units in the GSAP that are too small for a $0.5° \times 0.5°$ grid, we aggregate adjacent small units into a single unit that covers at least five $0.5° \times 0.5°$ grids (approximately 15,000 km^2) within each country and omit the isolated small units such as the Cayman Islands. Finally, 843 subnational units are kept in the GSAP, which cover 169 countries.

We investigate the influence of four hydroclimatic anomalies, including convective available potential energy (CAPE), vertically integrated moisture divergence (VIMD), vapor pressure deficit (VPD), and PET, on the drought-to-downpour weather whiplashes based on odd ratios calculated by fitting a logistic regression (Li et al., 2020; Mukherjee et al., 2023; Varga & Breuer, 2022). The logistic regression is fitted using the binary sequence of the last months of drought events as the independent variable (X) and that of months when downpours occur as the dependent variable (Y) with Z as the confounding variable. The odd ratio is given as $\exp(\beta)$, where β is the regression coefficient of the logit model, such that $\exp(\beta) > 1$ and $\exp(\beta) < 1$ indicate a multiplicative increase and decrease, respectively, in the odds of a downpour for a given drought and per unit increase in hydroclimatic variables or confounders (here, standardized anomalies of CAPE, VIMD, VPD, and PET).

3. Historical Characteristics of Drought-To-Downpour Events

Before assessing the drought-to-downpour events, we examine historical changes in the interval from drought to downpour (see Method and a schematic in Figure S1 in Supporting Information S1) and find a statistically significant ($P < 0.05$) decrease globally during the period of 1955–2014 for all three data sets (see Figure 1a for R95p and Figure S2 in Supporting Information S1 for R99p). The magnitude of estimated slope suggests a decrease of

6.6–16 days in the interval from droughts to R95p downpours during the study period for all three data sets, with a decadal decline of 1.1–2.5 days (Figure 1a). Such a decrease is 33–102 days with a decadal decline of 5.5–17 days if the downpour is defined as R99p (Figure S2a in Supporting Information S1). Such a decrease may further enhance the likelihood of abrupt shift from drought to downpour, leading to significant drought-to-downpour events (i.e., shift from drought to downpour within a month). We find that such drought-to-downpour events frequently occur in East Asia, Southeast Asia, Central Africa, Southern Brazil, Amazon Basin, Eastern United States, and Southern Europe (Figure 1b). Particularly, Southern Brazil, East Asia, and Eastern United States not only are the high-frequency regions but also show a relatively high probability of abrupt shift from drought to downpour (i.e., a relatively high percentage of droughts followed by downpours within a month), with more than 80% of droughts abruptly shifting to downpours within a month during the period of 1955–2014 (Figure 1c). These are also the regions where multiple high-impact events have been reported (Chaves & Ennes, 2021; Migiro, 2013; ReliefWeb, 2010). For example, Southern Brazil, one of the regions that are most vulnerable to droughts and downpours, experienced remarkably dry conditions from January 2014 to February 2015 followed by a downpour in 2015, which affected over 200,000 people across the states of Rio Grande do Sul and Santa Catarina in Southern Brazil (Geirinhas et al., 2021).

We also use a bootstrap resampling test to assess whether the observed drought-to-downpour probability is significantly higher than expected under independence between drought and downpour occurrences. The bootstrap resampling test compares the drought-to-downpour probability detected from the data product and 1,000 synthetic data sets. The synthetic data sets are generated by separately shuffling the observed binary time series of drought and downpour at the monthly scale (see Text S3 in Supporting Information S1). The observed drought-to-downpour probability is significantly ($P < 0.05$) higher than expected under independence between drought and downpour occurrences over 42% of global land area based on three data products (see the stippling in Figure 1c). This indicates that the abrupt shift from drought to downpour cannot be a pure coincidence. The occurrence of drought and downpour has a strong temporal dependence, which increases the global average probability of abrupt shift from 20%−29% to 37%−48% (Figure 1d). Such increases are nearly double (from 5%−8% to 11%−18%) for the abrupt shift from drought to heavy downpour (R99p) (Figure S2d in Supporting Information S1).

4. Growing Poverty Exposure to Drought-To-Downpour Events

Figure 2a shows that approximately 60% of global land area shows increases in the frequency of drought-to-downpour events between the early and later periods (1955–1984 and 1985–2014). These regions are home to approximately 4 billion people, mainly located in Africa, East Asia, Southern Europe, Southeastern Brazil, and the Arabian Peninsula, nearly 30% of which (1.22 billion) live in poverty (i.e., on less than $5.50 per day). Our results also show that there is a significant ($P < 0.05$) correlation between median multiplicative changes of drought-to-downpour events and the share of population living in poverty (i.e., on less than $5.50 per day) (see Figure 2b). Specifically, the frequency of drought-to-downpour events shows little change (i.e., Δ drought-to-downpour frequency close to 1) at the locations with poverty rates lower than 10%. In comparison, locations with poverty rates higher than 90% experience approximately 50% increases (i.e., Δ drought-to-downpour frequency equals 1.5), on average, in the frequency of drought-to-downpour events. For example, our estimates show that Mozambique experiences an 80% increase in drought-to-downpour events and more than 90% of population in Mozambique live in poverty. Among the top 10 countries in terms of multiplicative changes in drought-to-downpour events, seven have more than 70% of population living in poverty (Figure 2c).

We find that the poorest 20% of the world's population have experienced a statistically significant ($P < 0.05$) increase in the occurrence of drought-to-downpour events based on three data products during the period of 1980–2010 (Figure 3a and Figure S4 in Supporting Information S1). The magnitude of estimated slope suggests an increase of 24%–48% in the frequency of drought-to-downpour events during the study period, with an annual growth of 0.8%–1.6% (Figures S3 and S4 in Supporting Information S1). Such a significant increase, however, is not observed for the remaining wealthiest 80% of the world's population ($P = 0.08$). Climate simulations also show that the poorest 20% experienced a statistically significant ($P < 0.05$) increase in the frequency of drought-to-downpour events, with the ensemble-mean growth rate similar to those observed (see Figure 3b for CMIP5 and Figure S21 in Supporting Information S1 for CMIP6). The CMIP5 ensemble also resembles the insignificant changes in the frequency of observed drought-to-downpour events experienced by the wealthiest 80%

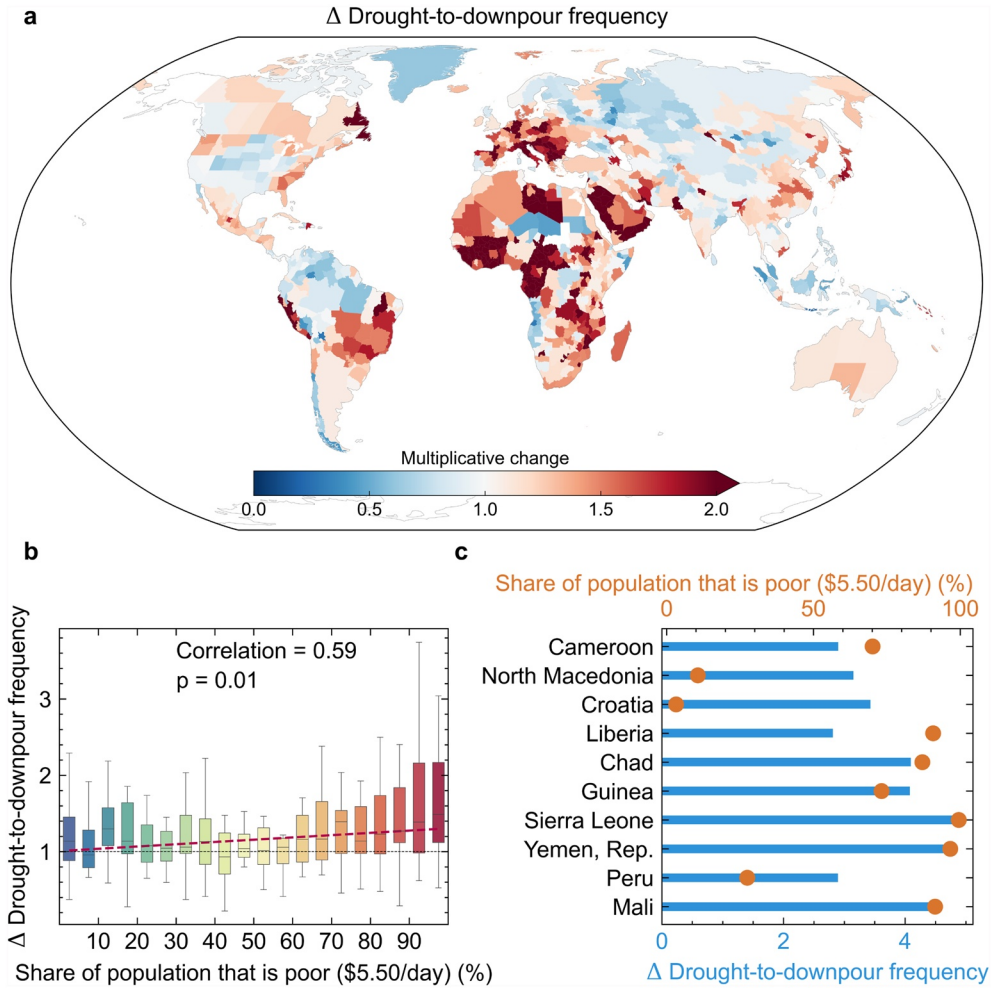

Figure 2. Drought-to-downpour events and poverty. (a) Observed multiplicative change from the early period (1955–1984) to the later period (1985–2014) in the frequency of drought-to-downpour events at the subnational level. (b) Global interrelationships between the share of population that is poor ($5.5 per day) and changes in the frequency of drought-to-downpour events. Box extents are at the 25th and 75th percentiles with Tukey whiskers. The red dashed line represents the fitted linear regression between poverty rates (*x*-axis) and median values of drought-to-downpour change (*y*-axis). The slope and p-value of the linear regression are shown. (c) The horizontal bar chart shows the 10 countries with the highest multiplicative changes of drought-to-downpour frequency, while the orange scatter plot shows the corresponding share of population that is poor ($5.5 per day).

(Figure S5 in Supporting Information S1). Here we merge the years 2006–2010 from the RCP4.5 simulations with the years 1980–2005 from the historical simulations since the trends in the probability of drought-to-downpour events under different emission scenarios are almost identical for the first two decades of the 21st century (Figure S6 in Supporting Information S1). Such divergent trends in the frequency of drought-to-downpour events experienced by poor and non-poor people are not affected by drought thresholds and extreme precipitation indices chosen to identify drought-to-downpour events (Figure S7 in Supporting Information S1).

We also find that the poverty exposure to drought-to-downpour events is projected to increase in the late twenty-first century relative to the late twentieth century. This is shown through aggregating locations by income decile and by graphing the local fraction of population exposed to a high drought-to-downpour risk for SSP2-4.5 and SSP5-8.5, respectively (see Figures 3c and 3d for CMIP5, Figure S8 in Supporting Information S1 for CMIP6, and Figure S9 in Supporting Information S1 for CESM-LENS). Here, the high drought-to-downpour risk is defined as over 80% of droughts abruptly shifting to downpours. The fraction of populations exposed to the high drought-to-downpour risk increases most for people from the poorer income deciles, with a nearly fivefold increase under SSP5-8.5. Such an increase is not significant for people from the wealthier income deciles.

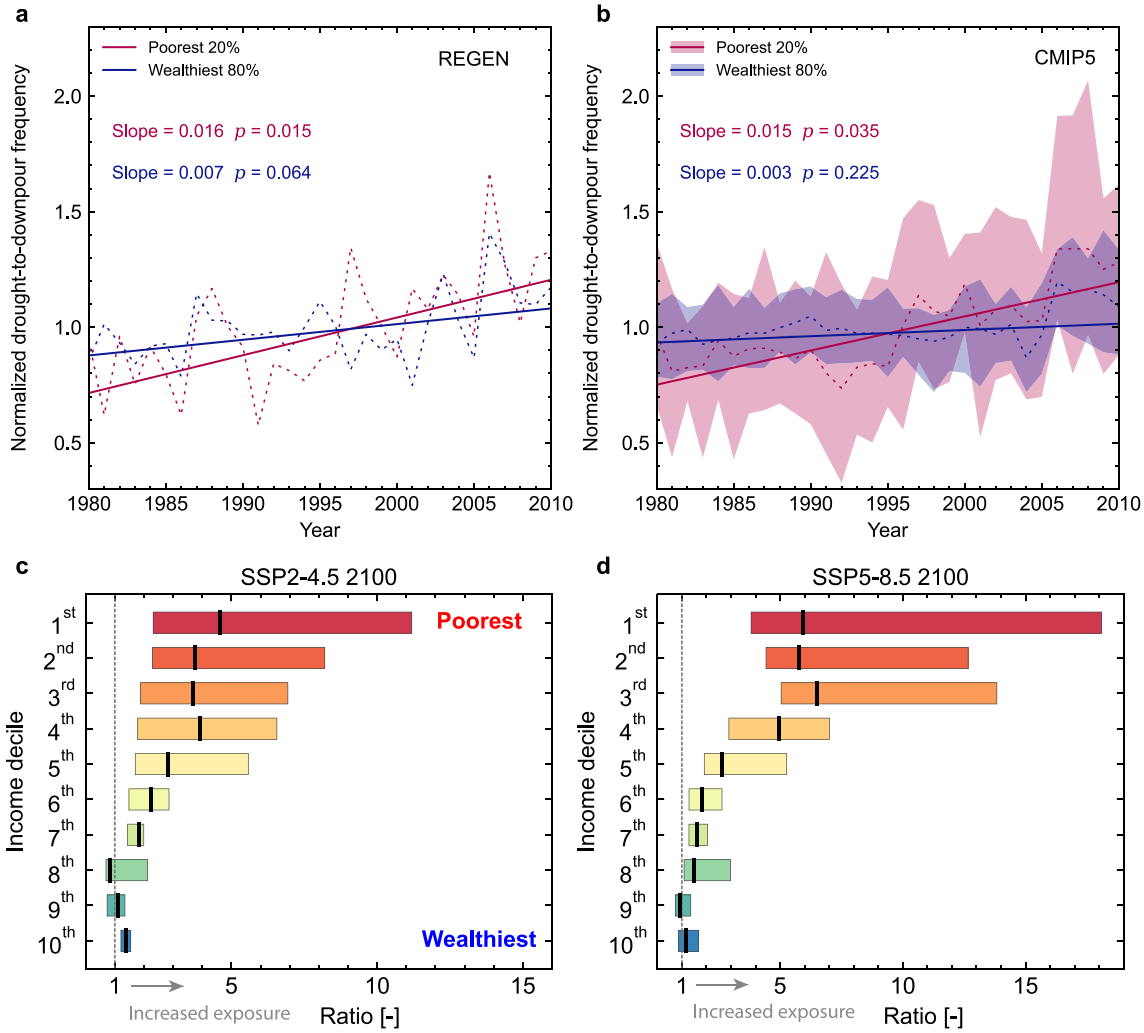

Figure 3. Time series of annual drought-to-downpour events generated from (a) the REGEN product and (b) CMIP5 simulations for the poorest 20% (red) and the wealthiest 80% (blue) regions of the world. The time series were normalized by calculating annual values as a fraction of the 1980–2010 local mean. The spatial distribution of the poorest 20% is shown in Figure S4a in Supporting Information S1. Dashed lines represent annual values from data products and ensemble mean; solid lines represent the linear trend; the lower and upper bounds of the colored shading refer to 2.5th and 97.5th percentile estimates, respectively. The slope (unit: year^{-1}) is the linear trend based on the Sen's slope estimator; and the *p*-value is the trend significance using a MK test. The fraction of (c) the poorest 20% and (d) the wealthiest 80% worldwide exposed to the drought-to-downpour probability of at least 80% under historical (1955–2004) and future (2051–2100) climates. Gridded data sets of population and GDP in 2000 and 2100 under SSP2 and SSP5 are taken from Gao (2020) and Murakami et al. (2021), respectively. Box extents are at the 25th and 75th percentiles with Tukey whiskers.

5. Changes in Processes Responsible for Drought-To-Downpour Events

We find that CAPE and VIMD show positive influences (odd ratio >2) on the odds of drought-to-downpour events mainly in tropical regions (Figures 4a and 4b). A higher value of CAPE means the atmosphere is more unstable and would therefore produce a stronger updraft that characterizes a storm's early development, and the intense water vapor transport (a high VIMD value) is likely to provide fuels for the occurrence of drought-to-downpour events. Some of these regions show a compounding influence of CAPE and VIMD, such as in Brazil, southeastern Africa, northern India, Southeast Asia, and northern Australia, where the values of odd ratio indicate that a simultaneous increase in CAPE and moisture convergence (negative VIMD) anomalies by one unit can yield 3–4 times increase in the odds of drought-to-downpour event cascade in these regions. Most of these regions show negative and strong influences of VPD, such as in central and northern North America, Russia, and Kazakhstan (Figure 4c). PET shows a positive but moderate influence (1 < odd ratio <2) and VPD shows a negligible influence in the majority of tropical regions (Figure 4d). The influence of PET is more dominant (odd ratio >3) in extratropical regions, including northern North America, Europe, and central and northern Asia.

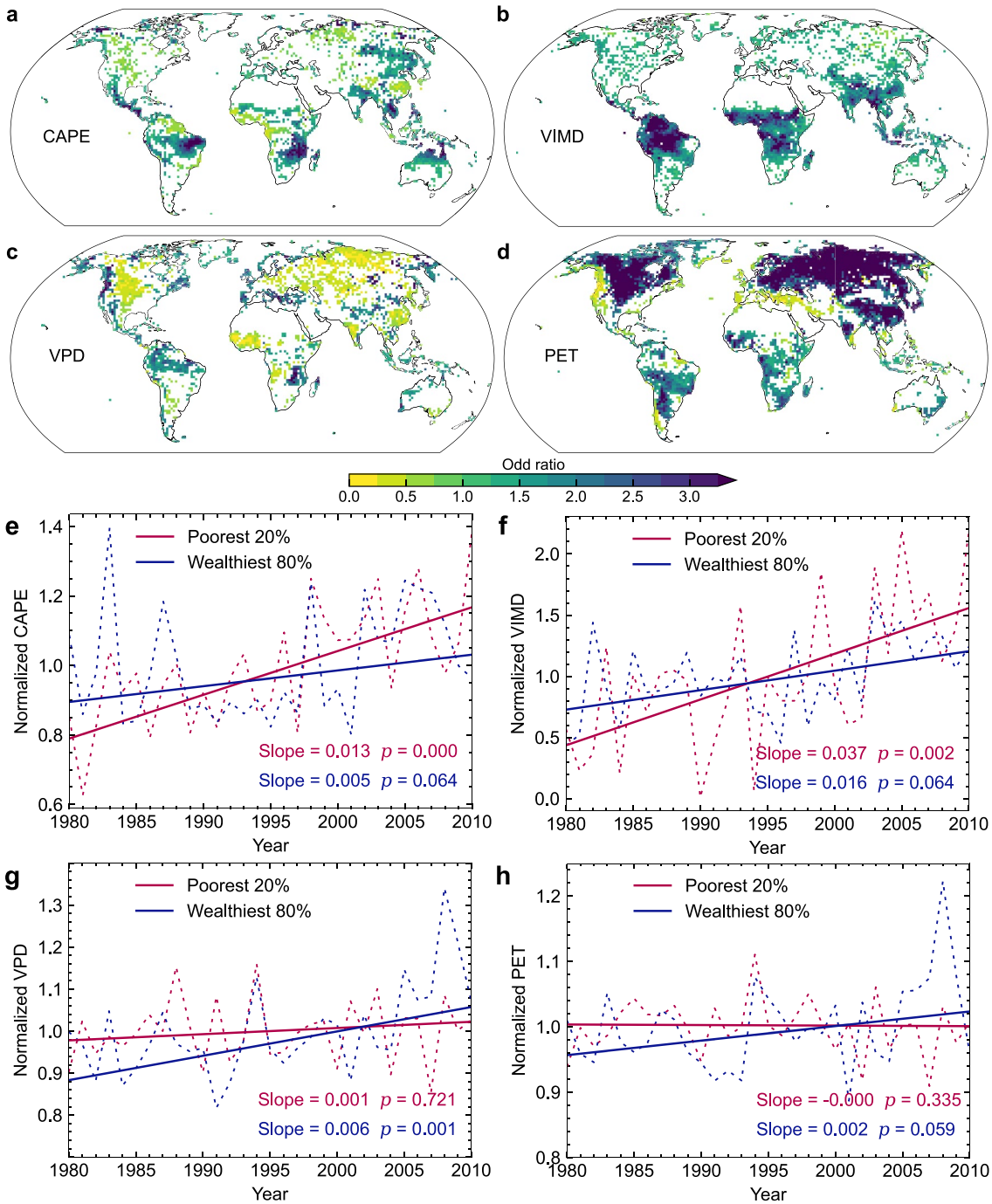

Figure 4. Spatial maps of statistically significant (at 95% confidence level) odd ratios (exp(β)) calculated by fitting the logistic regression model for the drought-downpour events associated with (a) CAPE, (b) VIMD, (c) VPD, and (d) PET. Normalized time series of averaged e CAPE, (f) VIMD, (g) VPD, and (h) PET during the drought termination period generated from the ERA5 reanalysis for the poorest 20% and the wealthiest 80% of the world. Dashed lines represent annual values and solid lines represent the linear trend. The *p*-value is the trend significance using a MK test.

We also find that changes in the four hydroclimatic anomalies may explain the different trends of drought-to-downpour events for the poorest 20% and the wealthiest 80% of the world's population. The CAPE and VIMD significantly ($P < 0.05$) increase at the drought termination period for the poorest 20% of the world's population (Figures 4e and 4f), thereby increasing the frequency of drought-to-downpour events for the corresponding area. Such increases, however, are not significant ($P > 0.05$) for the wealthiest 80%. Although the VPD shows a significant ($P < 0.05$) increase for the wealthiest 80% of the world's population (Figure 4g), it has a negative

impact on the drought-to-downpour occurrence for the extratropical region. The PET has a positive impact on the drought-to-downpour occurrence over the extratropical region, but it shows an insignificant ($P > 0.05$) change for the wealthiest 80% of the world's population (Figure 4h).

6. Discussion

The IPCC Sixth Assessment Report (AR6) suggests that developing countries need USD 140∼300 billion per year by 2030 for climate adaptation, but the increasing exposure of poor regions to the emerging weather whiplash was not considered in current climate assessment reports and adaptation strategies (Hallegatte & Rozenberg, 2017; Markkanen & Anger-Kraavi, 2019). Our results suggest that in addition to the well-known extreme events (Alizadeh et al., 2022; Mohanty & Simonovic, 2021; Winsemius et al., 2018), low-income regions and countries have likely been suffering significantly more than previously understood due to the increasing occurrence of drought-to-downpour events (Figure S20 in Supporting Information S1), and such increases are not detected for middle- and high-income regions. Low-income and vulnerable countries are very likely to need greater support than estimated by IPCC AR6 for adaptation to compound events. Climate adaptation of poor and vulnerable regions should address the emerging risk from drought-to-downpour events to avoid disproportionate burdens and additional damages, especially in East Asia, Southeast Asia, Central Africa, Southern Brazil, and Amazon Basin. Poverty exposure to more such compound events would have a higher potential to push vulnerable households into poverty and keep households poor than individual extreme events (Hallegatte et al., 2020; Hubacek et al., 2017; Rao et al., 2017), thereby reinforcing the inequalities. Although the COP27 established funding solutions for climate adaptation in low-income countries, international community's efforts toward climate justice would be hampered if drought-to-downpour events are not taken into account given their increasing poverty exposure and serious consequences (Green, 2016; Hallegatte et al., 2018). This could put at risk the achievement of the United Nations' Sustainable Development Goals which are to reduce poverty (Goal 1) and inequality within and between nations (Goal 10), as well as to take urgent actions to combat climate change impacts (Goal 13) (Codjoe & Atiglo, 2020; Diffenbaugh & Burke, 2019).

Identifying hydroclimatic anomalies associated with the exposure inequality of drought-to-downpour events is crucial to developing plausible measures aimed at reducing global inequality. Our findings reveal that the hydroclimatic anomalies in favor of the occurrence of drought-to-downpour events vary between poor and wealthy regions. The poor regions of the world tend to be located in the tropics and these regions show significant increases in atmospheric instability and water vapor transport that are in favor of the occurrence of drought-to-downpour events. In contrast, the wealthy regions of the world tend to be located in the extratropical regions, where the dominant hydroclimatic processes (e.g., evapotranspiration and vapor deficit) do not change toward a favorable condition for the occurrence of drought-to-downpour events. The poor regions of the world overlap with global monsoon regions where a statistically significant ($P < 0.01$) increase in the frequency of drought-to-downpour events is also detected, but such an increase is not exhibited in non-monsoon regions (Figure S10 in Supporting Information S1) (Wang et al., 2020; W. Zhang et al., 2021). The different changes in drought-to-downpour events for poor and wealthy regions may also result from changes in the drought frequency. Droughts show a statistically significant ($P = 0.016$) increase for the poor region of the world but do not show significant change for the wealthy region of the world (Figure S26 in Supporting Information S1). Previous studies also show that poor people are often disproportionally exposed to droughts (Winsemius et al., 2018). In addition, our findings also reveal that the exposure inequality remains under future socioeconomic pathways. Such an inequality may result from different changes in atmospheric conditions for the tropical and extratropical regions since the CMIP5 ensemble shows that atmospheric instability and water vapor transport are projected to significantly increase in tropical regions but show a smaller increase in extratropical regions between historical and future (RCP8.5) climates (Figure S11 in Supporting Information S1).

Our findings should be interpreted with caution since the scPDSI and extreme precipitation indices alone cannot offer a full picture of drought-to-downpour events. Specifically, daily rainfall exceeding the 95th and 99th percentiles may not completely reverse a significant drought since its many aspects end slowly and the legacy effects may persist for years. Significant seasonal rainfall may be required to end drought conditions, especially in regions vulnerable to multi-year droughts such as California and Australia (Swain et al., 2018). However, extreme precipitation indices can act as a proxy for flash flood warning and capture the abrupt shift from drought to flood warnings in a matter of days together with the scPDSI (Figures S14 and S15 in Supporting Information S1). Such

drought-to-downpour events leave little time for emergency management agencies to assess damages and prepare for the next hazard, especially for those low-income countries with limited capacities for forecasting and early warning. In comparison with the drought-to-downpour events, compound drought and downpour may not lead to significant water-related hazards (e.g., flash floods), but rather alleviate the ongoing droughts (see details in Text S4 in Supporting Information S1). We did not account for compound drought and downpour because the drought-to-downpour events may be more impactful as the ground at the drought termination period is more likely to become parched than that at the drought onset and development periods, which prevents rain from saturating the ground, thereby enhancing the risk of flash flooding (Figure S25 in Supporting Information S1). By using poverty rates at the subnational administrative level, we assume that hazard exposure is uniform across income groups within a given area. This may result in an overestimation of exposed populations for the locations with substantial socioeconomic inequality but does not affect the results regarding the connection between poverty incidence and drought-to-downpour events. In addition, although we use a logistic regression to understand the influences of the different processes on the occurrence of drought-to-downpour events, correlations between the different physical processes would violate the assumption of logistic regression, which may affect the analysis result and require futher investigation in the future.

Data Availability Statement

All data sets used in this study are publicly available. The REGEN precipitation product is available at Contractor et al. (2019). The ERA5 data set is available at Hersbach et al. (2023), and CAPE, VIMD, and VPD are derived from it. Princeton University's global land surface model data is available at Sheffield et al. (2006). The CRU data is available at Harris and Jones (2020). The CMIP5/6 model outputs are available at Taylor et al. (2012) and Eyring et al. (2016). The CESM-LENS model output is available at Kay et al. (2015). The population density map (WorldPop-2000) is publicly available at Tatem (2017). The GDP per capita data set is available at Kummu et al. (2020). Relevant processed data is stored at B. Zhang (2023).

Acknowledgments
This research was supported by the Hong Kong Research Grants Council Early Career Scheme (Grant 25222319) and the Hong Kong Polytechnic University (Grant P0045957, P0043040). J.Z. acknowledges the Helmholtz Initiative and Networking Fund (Young Investigator Group COMPOUNDX; grant agreement no. VH-NG-1537).

References

Ahmadalipour, A., Moradkhani, H., Castelletti, A., & Magliocca, N. (2019). Future drought risk in Africa: Integrating vulnerability, climate change, and population growth. *Science of the Total Environment*, *662*, 672–686. https://doi.org/10.1016/j.scitotenv.2019.01.278

Ahmadalipour, A., Moradkhani, H., & Kumar, M. (2019). Mortality risk from heat stress expected to hit poorest nations the hardest. *Climatic Change*, *152*(3–4), 569–579. https://doi.org/10.1007/s10584-018-2348-2

Alizadeh, M. R., Abatzoglou, J. T., Adamowski, J. F., Prestemon, J. P., Chittoori, B., Akbari Asanjan, A., & Sadegh, M. (2022). Increasing heat-stress inequality in a warming climate. *Earth's Future*, *10*(2), e2021EF002488. https://doi.org/10.1029/2021EF002488

Baez, J. E., Caruso, G., & Niu, C. (2020). Extreme weather and poverty risk: Evidence from multiple shocks in Mozambique. *Economics of Disasters and Climate Change*, *4*(1), 103–127. https://doi.org/10.1007/s41885-019-00049-9

Batibeniz, F., Ashfaq, M., Diffenbaugh, N. S., Key, K., Evans, K. J., Turuncoglu, U. U., & Önol, B. (2020). Doubling of U.S. population exposure to climate extremes by 2050. *Earth's Future*, *8*(4), e2019EF001421. https://doi.org/10.1029/2019EF001421

Brida, A. B., Owiyo, T., & Sokona, Y. (2013). Loss and damage from the double blow of flood and drought in Mozambique. *International Journal of Global Warming*, *5*(4), 514–531. https://doi.org/10.1504/IJGW.2013.057291

Callahan, C. W., & Mankin, J. S. (2022). Globally unequal effect of extreme heat on economic growth. *Science Advances*, *8*(43), eadd3726. https://doi.org/10.1126/sciadv.add3726

Chaves, L., & Ennes, J. (2021). From flood to drought, Brazil's Acre state swings between weather extremes. Retrieved from https://news.mongabay.com/2021/10/from-flood-to-drought-brazils-acre-state-swings-between-weather-extremes/

Chen, H., & Wang, S. (2022). Accelerated transition between dry and wet periods in a warming climate. *Geophysical Research Letters*, *49*(19), e2022GL099766. https://doi.org/10.1029/2022GL099766

Codjoe, S. N. A., & Atiglo, D. Y. (2020). The implications of extreme weather events for attaining the Sustainable Development Goals in sub-Saharan Africa. *Frontiers in Climate*, *2*, 592658. https://doi.org/10.3389/fclim.2020.592658

Collenteur, R. A., de Moel, H., Jongman, B., & Di Baldassarre, G. (2015). The failed-levee effect: Do societies learn from flood disasters? *Natural Hazards*, *76*(1), 373–388. https://doi.org/10.1007/s11069-014-1496-6

Contractor, S., Donat, M. G., Alexander, L. V., Ziese, M., Meyer-Christoffer, A., Schneider, U., et al. (2019). Rainfall estimates on a gridded network based on all station data v1-2019 [Dataset]. NCI Data Catalog. https://doi.org/10.25914/5ca4c380b0d44

Deser, C., Lehner, F., Rodgers, K. B., Ault, T., Delworth, T. L., DiNezio, P. N., et al. (2020). Insights from Earth system model initial-condition large ensembles and future prospects. *Nature Climate Change*, *10*(4), 277–286. https://doi.org/10.1038/s41558-020-0731-2

Diffenbaugh, N. S., & Burke, M. (2019). Global warming has increased global economic inequality. *Proceedings of the National Academy of Sciences*, *116*(20), 9808–9813. https://doi.org/10.1073/pnas.1816020116

Eckstein, D., Künzel, V., & Schäfer, L. (2021). *Global climate risk index 2021* (p. 28). Germanwatch e.V. Retrieved from https://www.germanwatch.org/sites/default/files/Global%20Climate%20Risk%20Index%202021_2.pdf

Eyring, V., Bony, S., Meehl, G. A., Senior, C. A., Stevens, B., Stouffer, R. J., & Taylor, K. E. (2016). The coupled model intercomparison project phase 6 (CMIP6) [Dataset]. ESGF-NODE. Retrieved from https://esgf-node.llnl.gov/projects/cmip6/

Gao, J. (2020). *Global 1-km downscaled population base year and projection grids based on the shared socioeconomic pathways, Revision 01*. NASA Socioeconomic Data and Applications Center (SEDAC). https://doi.org/10.7927/q7z9-9r69

Gazzotti, P., Emmerling, J., Marangoni, G., Castelletti, A., van der Wijst, K.-I., Hof, A., & Tavoni, M. (2021). Persistent inequality in economically optimal climate policies. *Nature Communications*, *12*(1), 3421. https://doi.org/10.1038/s41467-021-23613-y

Geirinhas, J. L., Russo, A., Libonati, R., Sousa, P. M., Miralles, D. G., & Trigo, R. M. (2021). Recent increasing frequency of compound summer drought and heatwaves in Southeast Brazil. *Environmental Research Letters*, *16*(3), 034036. https://doi.org/10.1088/1748-9326/abe0eb

Green, D. (2016). The spatial distribution of extreme climate events, another climate inequity for the world's most vulnerable people. *Environmental Research Letters*, *11*(9), 091002. https://doi.org/10.1088/1748-9326/11/9/091002

Hallegatte, S., Fay, M., & Barbier, E. B. (2018). Poverty and climate change: Introduction. *Environment and Development Economics*, *23*(3), 217–233. https://doi.org/10.1017/S1355770X18000141

Hallegatte, S., & Rozenberg, J. (2017). Climate change through a poverty lens. *Nature Climate Change*, *7*(4), 250–256. https://doi.org/10.1038/nclimate3253

Hallegatte, S., Vogt-Schilb, A., Rozenberg, J., Bangalore, M., & Beaudet, C. (2020). From poverty to disaster and back: A review of the literature. *Economics of Disasters and Climate Change*, *4*(1), 223–247. https://doi.org/10.1007/s41885-020-00060-5

Harris, I., & Jones, P. D. (2020). CRU TS4.03: Climatic research unit (CRU) time-series (TS) version 4.03 of high-resolution gridded data of month-by-month variation in climate [Dataset]. Centre for Environmental Data Analysis. https://doi.org/10.5285/10d3e3640f004c578403419aac167d82

He, X., & Sheffield, J. (2020). Lagged compound occurrence of droughts and pluvials globally over the past seven decades. *Geophysical Research Letters*, *47*(14), e2020GL087924. https://doi.org/10.1029/2020GL087924

Hersbach, H., Bell, B., Berrisford, P., Biavati, G., Horányi, A., Muñoz Sabater, J., et al. (2023). ERA5 hourly data on single levels from 1940 to present [Dataset]. Copernicus Climate Change Service (C3S) Climate Data Store (CDS). https://doi.org/10.24381/cds.adbb2d47

Hersbach, H., Bell, B., Berrisford, P., Hirahara, S., Horányi, A., Muñoz-Sabater, J., et al. (2020). The ERA5 global reanalysis. *Quarterly Journal of the Royal Meteorological Society*, *146*(730), 1999–2049. https://doi.org/10.1002/qj.3803

Hubacek, K., Baiocchi, G., Feng, K., & Patwardhan, A. (2017). Poverty eradication in a carbon constrained world. *Nature Communications*, *8*(1), 912. https://doi.org/10.1038/s41467-017-00919-4

Kay, J. E., Deser, C., Phillips, A., Mai, A., Hannay, C., Strand, G., et al. (2015). The community earth system model (CESM) large ensemble project [Dataset]. CESM-UCAR. Retrieved from https://www.cesm.ucar.edu/projects/community-projects/LENS/data-sets.html

Kendall, M. G. (1975). *Rank correlation methods* (4th ed.). Charles Griffin.

King, A. D., & Harrington, L. J. (2018). The inequality of climate change from 1.5 to 2°C of global warming. *Geophysical Research Letters*, *45*(10), 5030–5033. https://doi.org/10.1029/2018GL078430

Kummu, M., Taka, M., & Guillaume, J. H. A. (2020). Data from: Gridded global datasets for gross domestic product and human development index over 1990-2015 [Dataset]. Dryad. https://doi.org/10.5061/dryad.dk1j0

Li, F., Chavas, D. R., Reed, K. A., & Dawson, D. T. (2020). Climatology of severe local storm environments and synoptic-scale features over North America in ERA5 reanalysis and CAM6 simulation. *Journal of Climate*, *33*(19), 8339–8365. https://doi.org/10.1175/JCLI-D-19-0986.1

Markkanen, S., & Anger-Kraavi, A. (2019). Social impacts of climate change mitigation policies and their implications for inequality. *Climate Policy*, *19*(7), 827–844. https://doi.org/10.1080/14693062.2019.1596873

Masood, E., Tollefson, J., & Irwin, A. (2022). COP27 climate talks: What succeeded, what failed and what's next. *Nature*, *612*(7938), 16–17. https://doi.org/10.1038/d41586-022-03807-0

Migiro, K. (2013). With 62 dead, Kenya must end drought-flood cycle - Red Cross. Retrieved from https://news.trust.org/item/20130425095508-c7hi9/

Mohanty, M. P., & Simonovic, S. P. (2021). Understanding dynamics of population flood exposure in Canada with multiple high-resolution population datasets. *Science of the Total Environment*, *759*, 143559. https://doi.org/10.1016/j.scitotenv.2020.143559

Mukherjee, S., Mishra, A. K., Zscheischler, J., & Entekhabi, D. (2023). Interaction between dry and hot extremes at a global scale using a cascade modeling framework. *Nature Communications*, *14*(1), 277. https://doi.org/10.1038/s41467-022-35748-7

Murakami, D., Yoshida, T., & Yamagata, Y. (2021). Gridded GDP projections compatible with the five SSPs (shared socioeconomic pathways). *Frontiers in Built Environment*, *7*, 760306. https://doi.org/10.3389/fbuil.2021.760306

Parry, S., Marsh, T., & Kendon, M. (2013). 2012: From drought to floods in England and Wales. *Weather*, *68*(10), 268–274. https://doi.org/10.1002/wea.2152

Qing, Y., Wang, S., Yang, Z.-L., & Gentine, P. (2023). Soil moisture–atmosphere feedbacks have triggered the shifts from drought to pluvial conditions since 1980. *Communications Earth & Environment*, *4*(1), 254. https://doi.org/10.1038/s43247-023-00922-2

Rao, N. D., Van Ruijven, B. J., Riahi, K., & Bosetti, V. (2017). Improving poverty and inequality modelling in climate research. *Nature Climate Change*, *7*(12), 857–862. https://doi.org/10.1038/s41558-017-0004-x

ReliefWeb (2010). Drought followed by floods in central Africa. Retrieved from https://reliefweb.int/report/chad/drought-followed-floods-central-africa

Rentschler, J., Salhab, M., & Jafino, B. A. (2022). Flood exposure and poverty in 188 countries. *Nature Communications*, *13*(1), 1–11. https://doi.org/10.1038/s41467-022-30727-4

Roxy, M. K., Ghosh, S., Pathak, A., Athulya, R., Mujumdar, M., Murtugudde, R., et al. (2017). A threefold rise in widespread extreme rain events over central India. *Nature Communications*, *8*(1), 1–11. https://doi.org/10.1038/s41467-017-00744-9

Sen, P. K. (1968). Estimates of the regression coefficient based on Kendall's Tau. *Journal of the American Statistical Association*, *63*(324), 1379–1389. https://doi.org/10.1080/01621459.1968.10480934

Sheffield, J., Goteti, G., & Wood, E. F. (2006). Global meteorological forcing dataset for land surface modeling [Dataset]. Research Data Archive at the National Center for Atmospheric Research, Computational and Information Systems Laboratory. https://doi.org/10.5065/JV89-AH11

Simon, D., & Leck, H. (2015). Understanding climate adaptation and transformation challenges in African cities. *Current Opinion in Environmental Sustainability*, *13*, 109–116. https://doi.org/10.1016/j.cosust.2015.03.003

Simon Wang, S. Y., Yoon, J. H., Becker, E., & Gillies, R. (2017). California from drought to deluge. *Nature Climate Change*, *7*(7), 465–468. https://doi.org/10.1038/nclimate3330

Son, R., Wang, S. Y. S., Tseng, W. L., Barreto Schuler, C. W., Becker, E., & Yoon, J. H. (2020). Climate diagnostics of the extreme floods in Peru during early 2017. *Climate Dynamics*, *54*(1–2), 935–945. https://doi.org/10.1007/s00382-019-05038-y

Swain, D. L., Langenbrunner, B., Neelin, J. D., & Hall, A. (2018). Increasing precipitation volatility in twenty-first-century California. *Nature Climate Change*, *8*(5), 427–433. https://doi.org/10.1038/s41558-018-0140-y

Tatem, A. J. (2017). WorldPop, open data for spatial demography [Dataset]. WorldPop, *4*(1), 170004. https://doi.org/10.1038/sdata.2017.4

Taylor, K. E., Stouffer, R. J., & Meehl, G. A. (2012). The coupled model intercomparison project phase 5 (CMIP5) [Dataset]. NODE-ESGF. Retrieved from https://esgf-node.llnl.gov/projects/cmip5/

Varga, Á. J., & Breuer, H. (2022). Evaluation of convective parameters derived from pressure level and native ERA5 data and different resolution WRF climate simulations over Central Europe. *Climate Dynamics*, *58*(5–6), 1569–1585. https://doi.org/10.1007/s00382-021-05979-3

Wang, B., Jin, C., & Liu, J. (2020). Understanding future change of global monsoons projected by CMIP6 models. *Journal of Climate*, *33*(15), 6471–6489. https://doi.org/10.1175/JCLI-D-19-0993.1

Wing, O. E. J., Lehman, W., Bates, P. D., Sampson, C. C., Quinn, N., Smith, A. M., et al. (2022). Inequitable patterns of US flood risk in the Anthropocene. *Nature Climate Change*, *12*(2), 156–162. https://doi.org/10.1038/s41558-021-01265-6

Winsemius, H. C., Jongman, B., Veldkamp, T. I. E., Hallegatte, S., Bangalore, M., & Ward, P. J. (2018). Disaster risk, climate change, and poverty: Assessing the global exposure of poor people to floods and droughts. *Environment and Development Economics*, *23*(3), 328–348. https://doi.org/10.1017/S1355770X17000444

World Bank. (2021). *World Bank estimates based on data from the global subnational atlas of poverty (Global Mon)*. World Bank.

WorldPop (2020). WorldPop open population repository. Retrieved from https://wopr.worldpop.org/?SLE/

Yang, Y., Roderick, M. L., Zhang, S., McVicar, T. R., & Donohue, R. J. (2019). Hydrologic implications of vegetation response to elevated CO_2 in climate projections. *Nature Climate Change*, *9*(1), 44–48. https://doi.org/10.1038/s41558-018-0361-0

You, J., Wang, S., Zhang, B., Raymond, C., & Matthews, T. (2023). Growing threats from swings between hot and wet extremes in a warmer world. *Geophysical Research Letters*, *50*(14), e2023GL104075. https://doi.org/10.1029/2023GL104075

Zhang, B. (2023). Higher exposure of poorer people to emerging weather whiplash in a warmer world [Dataset]. Zenodo. https://doi.org/10.5281/zenodo.7750974

Zhang, W., Furtado, K., Wu, P., Zhou, T., Chadwick, R., Marzin, C., et al. (2021). Increasing precipitation variability on daily-to-multiyear time scales in a warmer world. *Science Advances*, *7*(31), eabf8021. https://doi.org/10.1126/sciadv.abf8021

Zscheischler, J., Martius, O., Westra, S., Bevacqua, E., Raymond, C., Horton, R. M., et al. (2020). A typology of compound weather and climate events. *Nature Reviews Earth & Environment*, *1*(7), 333–347. https://doi.org/10.1038/s43017-020-0060-z

Zscheischler, J., Westra, S., van den Hurk, B. J. J. M., Seneviratne, S. I., Ward, P. J., Pitman, A., et al. (2018). Future climate risk from compound events. *Nature Climate Change*, *8*(6), 469–477. https://doi.org/10.1038/s41558-018-0156-3